Solar Cycle Prediction and Reconstruction Using Spherical Advective Magnetic Flux Transport Codes

Dr. David H. Hathaway[1]
NASA/Ames Research Center

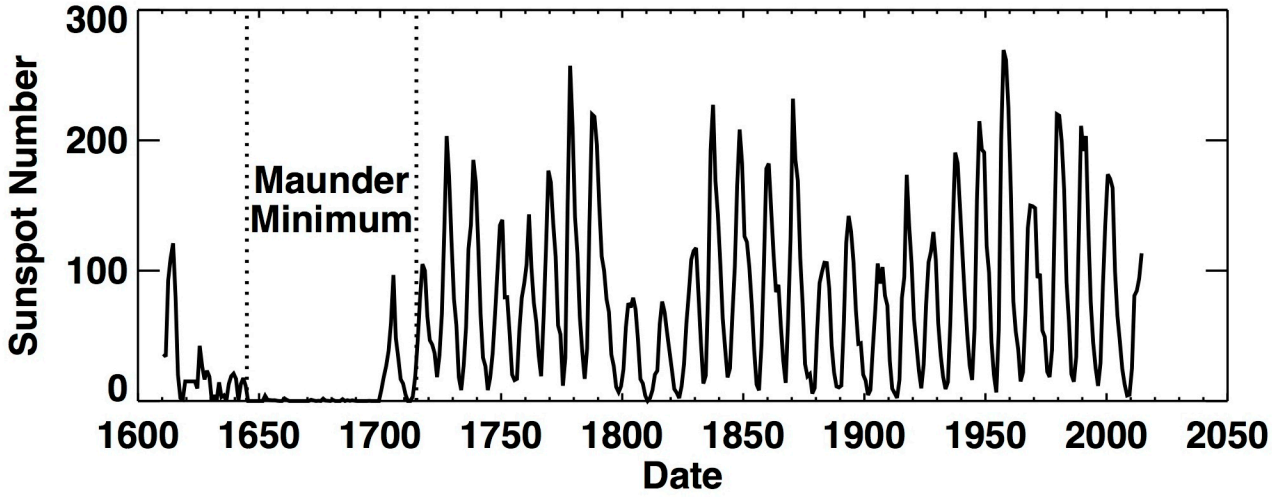

[1]With collaborators: Lisa Rightmire-Upton, Thibaud Teil, Nagi Mansour, Thomas Hartlep, and the Heliophysics Team

AMS Seminar Series, NASA Ames Research Center, November 3, 2015

Outline

Solar cycle characteristics

Producing the solar cycle – the solar dynamo

Polar magnetic fields – produce the next cycle

Surface magnetic flux transport – produce the polar fields

Measuring the surface flux transport flows

Reconstructing and predicting the cycle – caveat emptor

Solar Cycle Characteristics

Cycle Variability

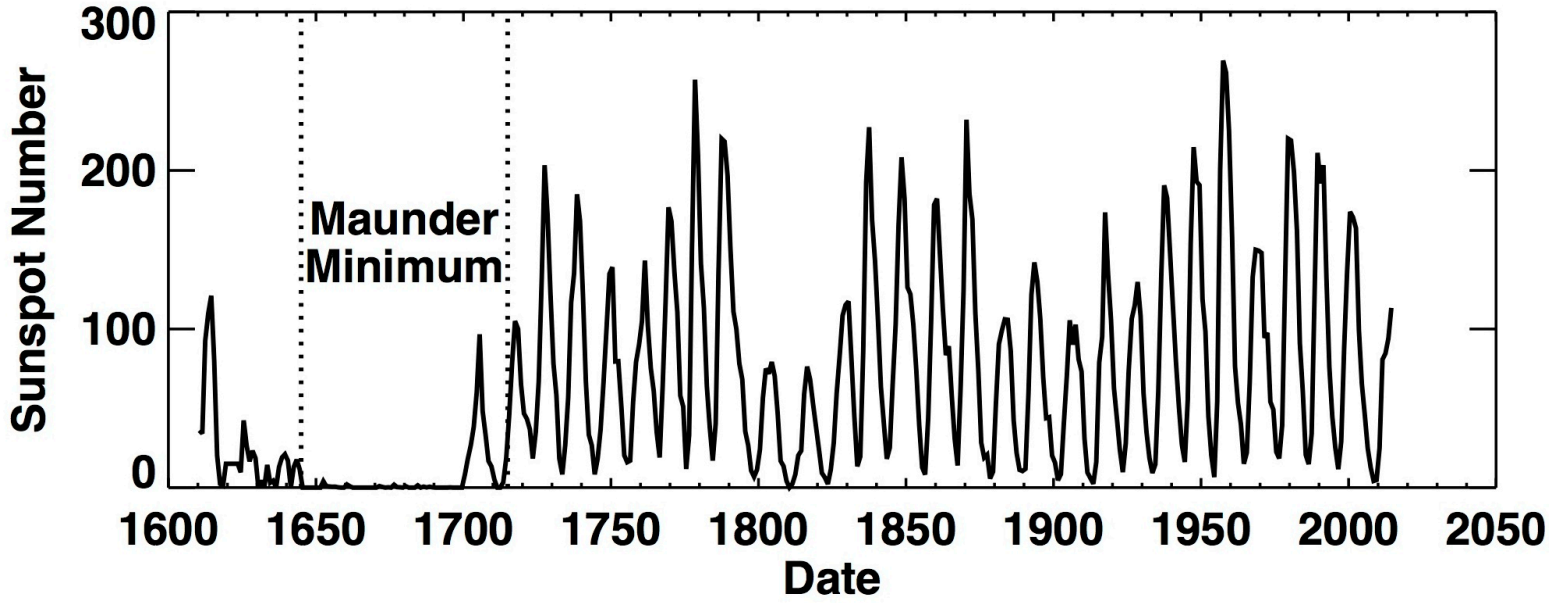

Yearly average of daily sunspot numbers (V2.0) since the invention of the telescope in 1610.

- **Cycle period ~11 years (9-14 years)**
- **Cycle amplitude ~ 150 (50-250)**
- **Maunder Minimum (no sunspots 1645-1715)**
- **Gleissberg Cycle (~100 year modulation of cycle amplitudes)**

Active Latitudes

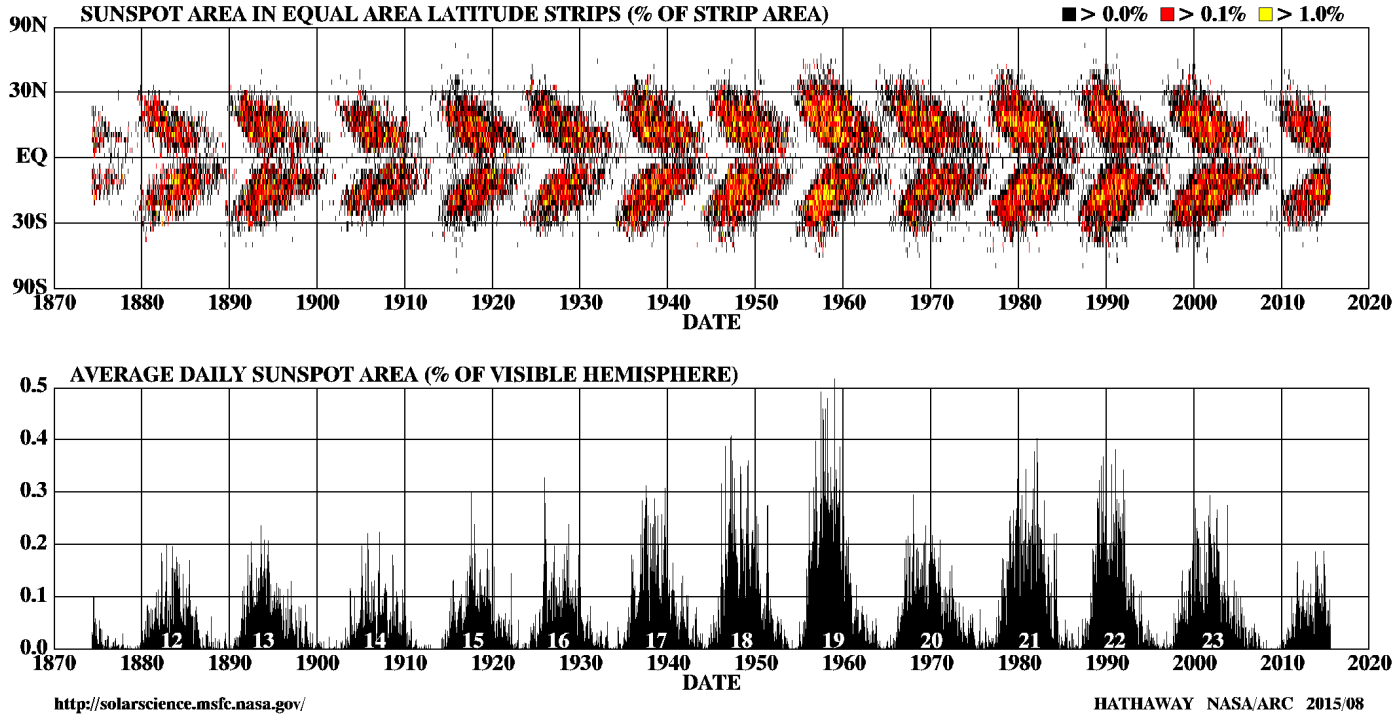

Monthly (27-day solar rotation) averages of daily sunspot area

- **Low-latitude sunspot zones on either side of the equator**
- **Zones drift toward the equator over each sunspot cycle**
- **Zones broaden as sunspot number/area increases**
- **Zones overlap at cycle minima**

Sunspot Numbers vs. Solar Activity

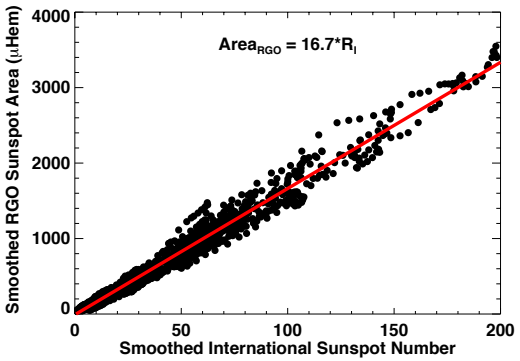

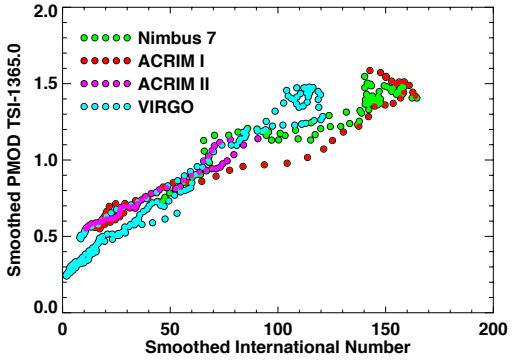

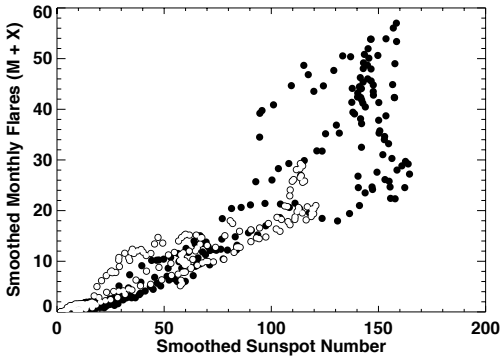

The number of sunspots is an historical indicator of solar activity, but is well correlated with other, more physical, quantities such as sunspot area, Total Solar Irradiance (TSI), and the number of M- and X-Class x-ray flares (*Hathaway, 2015*).

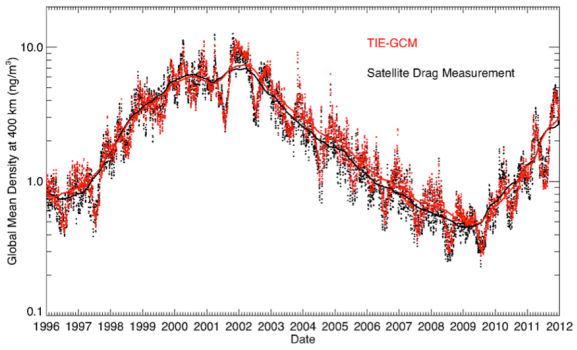

The irradiance of the Sun in the EUV/XUV varies by over an order of magnitude over a solar cycle. This radiation is absorbed by chemical species in Earth's upper atmosphere, the thermosphere, heating it and changing its density and consequent satellite drag by similar factors.

Cycle Shape in Time

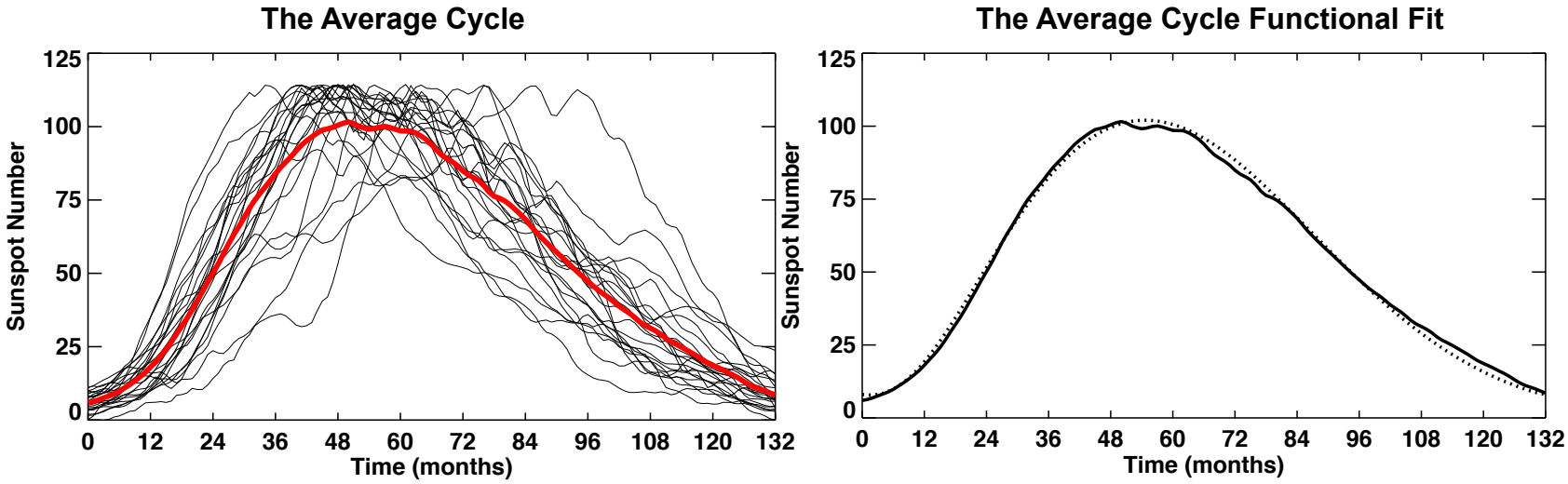

The average sunspot cycle (red curve) is asymmetric – rising to a maximum in 4 years and declining to minimum over the remaining 7 years. This shape is well fit with a parametric function:

$$F(t) = A\left(\frac{t-t_0}{b}\right)^3\left[\exp\left(\frac{t-t_0}{b}\right)^2 - c\right]^{-1}$$

with *c=0.71* and *b=b(A)* leaving a function of just t_0 and *A (Hathaway et al. 1994)*.

Active Latitude Drift

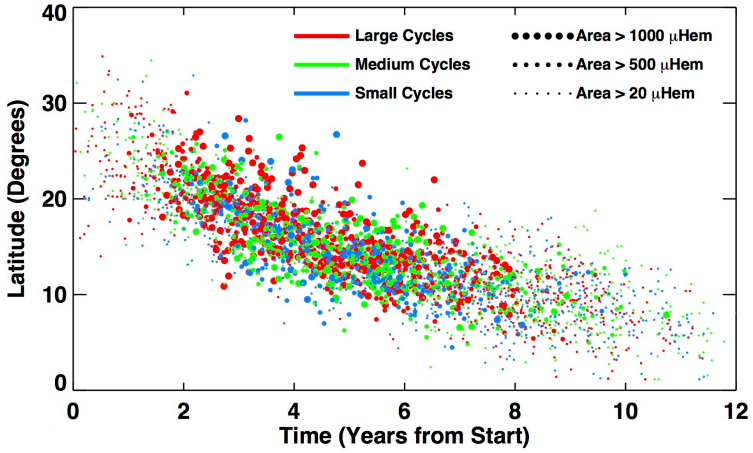

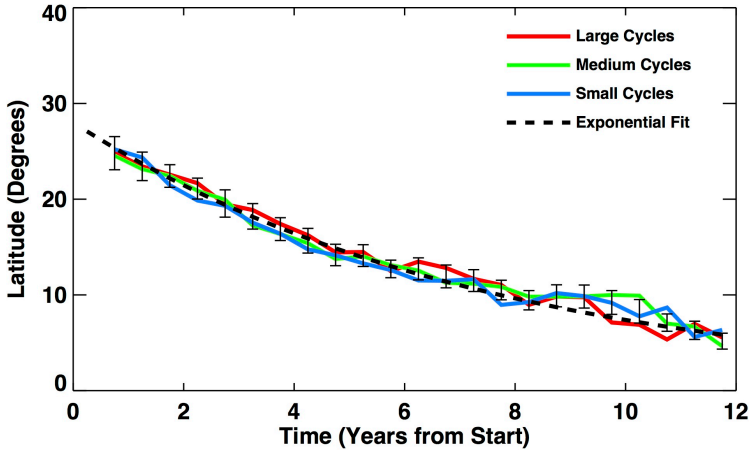

The active latitudes drift equatorward at the same rate and along the same path regardless of cycle size, when time is measured relative to the start time, t_0. This path is well represented by

$$\lambda(t) = 28° \exp[-(t - t_0)/90]$$

where time is measured in months (*Hathaway, 2011*).

Active Latitude Width

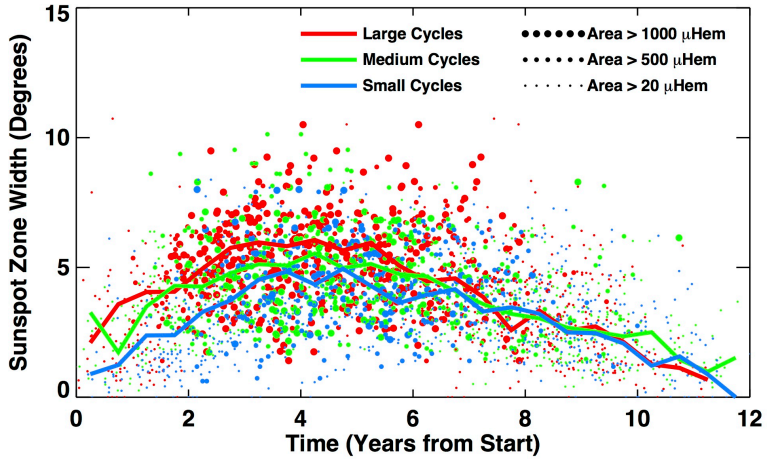

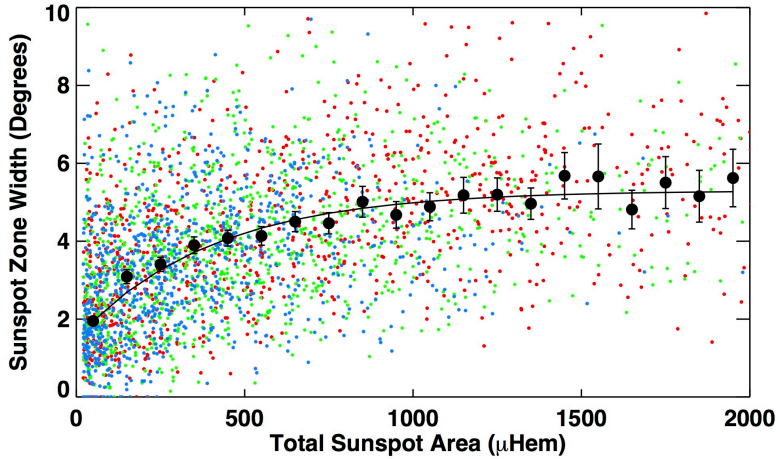

The width of the active latitude zones does vary with cycle strength but is a function of activity level (e.g. total sunspot area) only with the rms width given by

$$\sigma_\lambda(Area) = 1.5° + 3.8° \, [1 - \exp(-Area/400)]$$

where *Area* is the total sunspot area in μHem (*Hathaway, 2015*).

This gives a statistical prescription for the locations and sizes of sunspot groups over the course of a cycle as a function of cycle starting time, t_0, and cycle amplitude, *A*.

Predicting Activity in an Ongoing Cycle

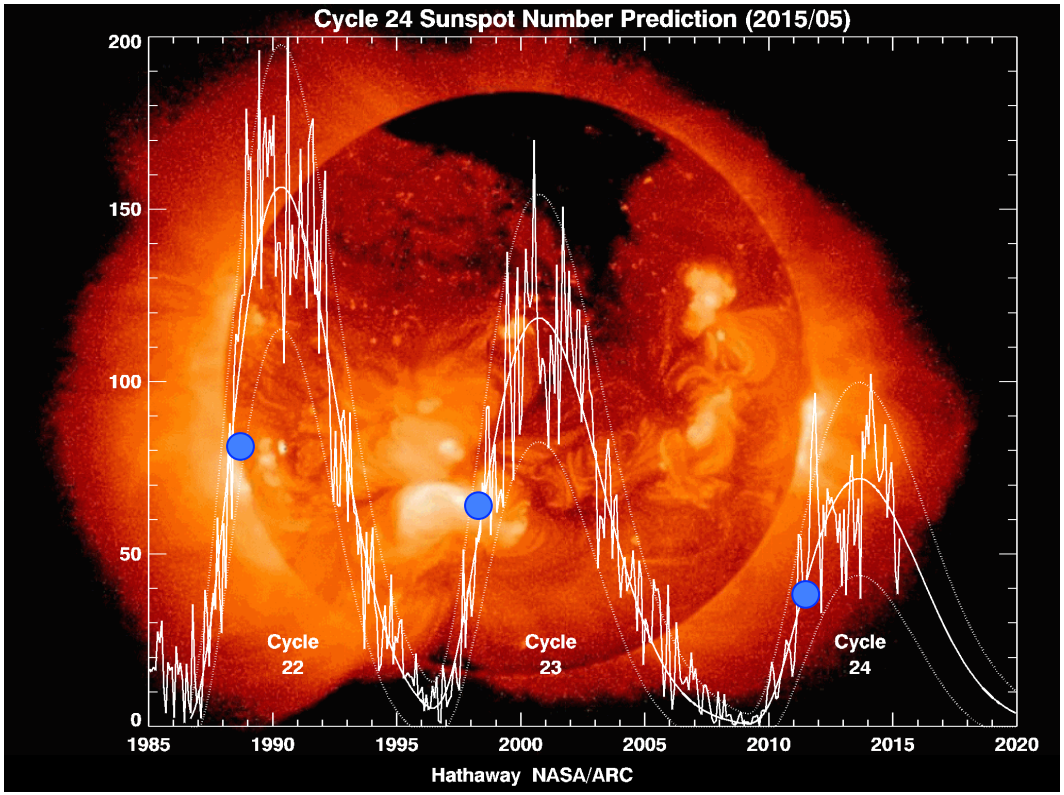

Reliable predictions of ongoing cycles have been made by fitting the observed monthly averaged sunspot numbers to this parametric function. These predictions become reliable 2-3 years after the cycle starts (blue dots at inflection points of curve).

Producing the Cycle – the Solar Dynamo

The Babcock-Leighton Dynamo

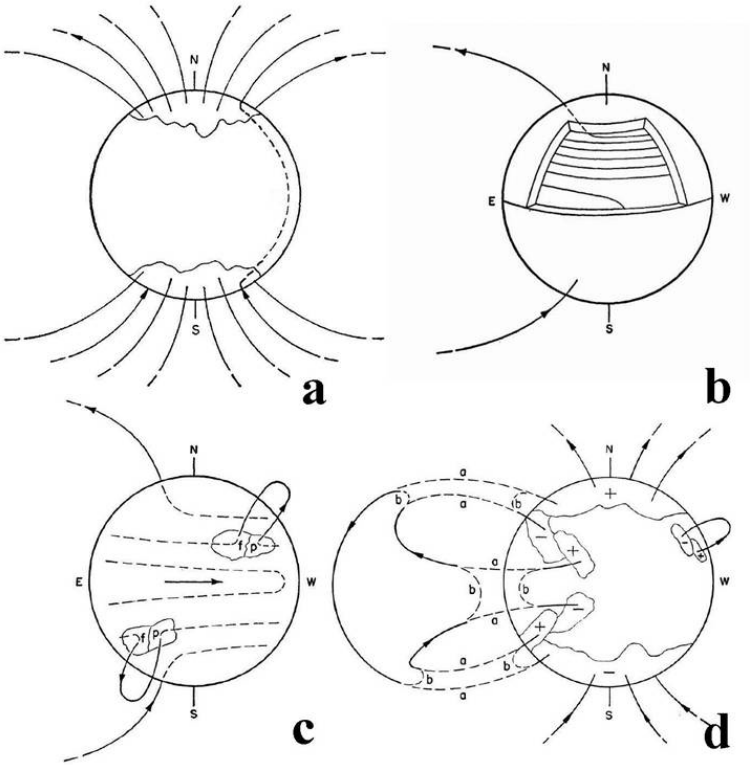

Babcock (1961)

a. Cycle starts with dipole field at minimum

b. Dipole field is stretched by differential rotation to produce azimuthal, toroidal field

c. Toroidal field becomes strong enough to become buoyant and rise through the surface to form bipolar active regions with a tilt from the azimuthal direction

d. Surface flux transport carries high-latitude (predominantly) following polarity flux to the poles

a. New (reversed polarity) polar fields are the seeds of the next cycle

Active Region Tilt – Joy's Law

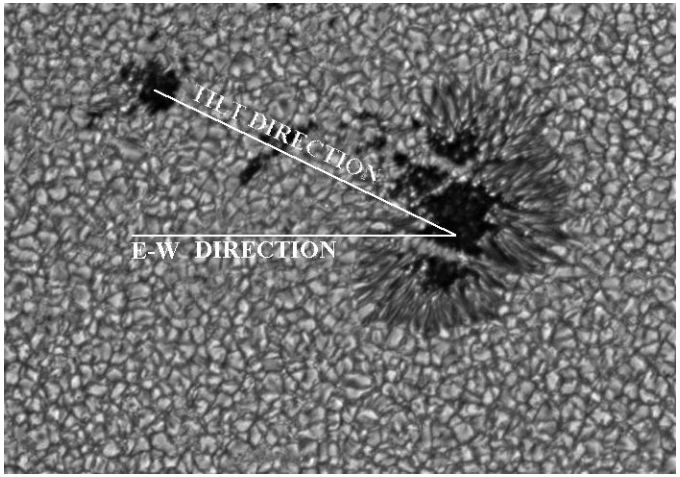

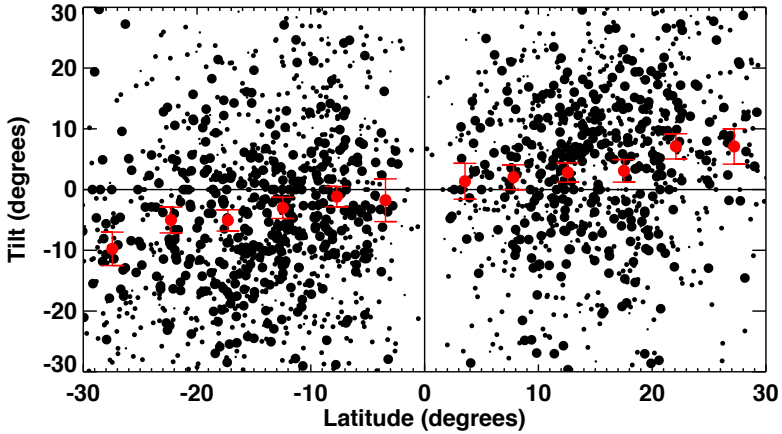

Sunspots emerge in groups with the sunspots aligned in a roughly east-west direction.

***Hale et al. (1919)* noted that the preceding sunspots had one magnetic polarity while the following sunspots had the opposite polarity.**

In that paper, Joy noted that sunspot groups have a slight tilt with the following polarity sunspots closer to the poles.

These tilts have a lot of scatter, but the average tilt is found to increase with latitude.

The Dynamo Observed

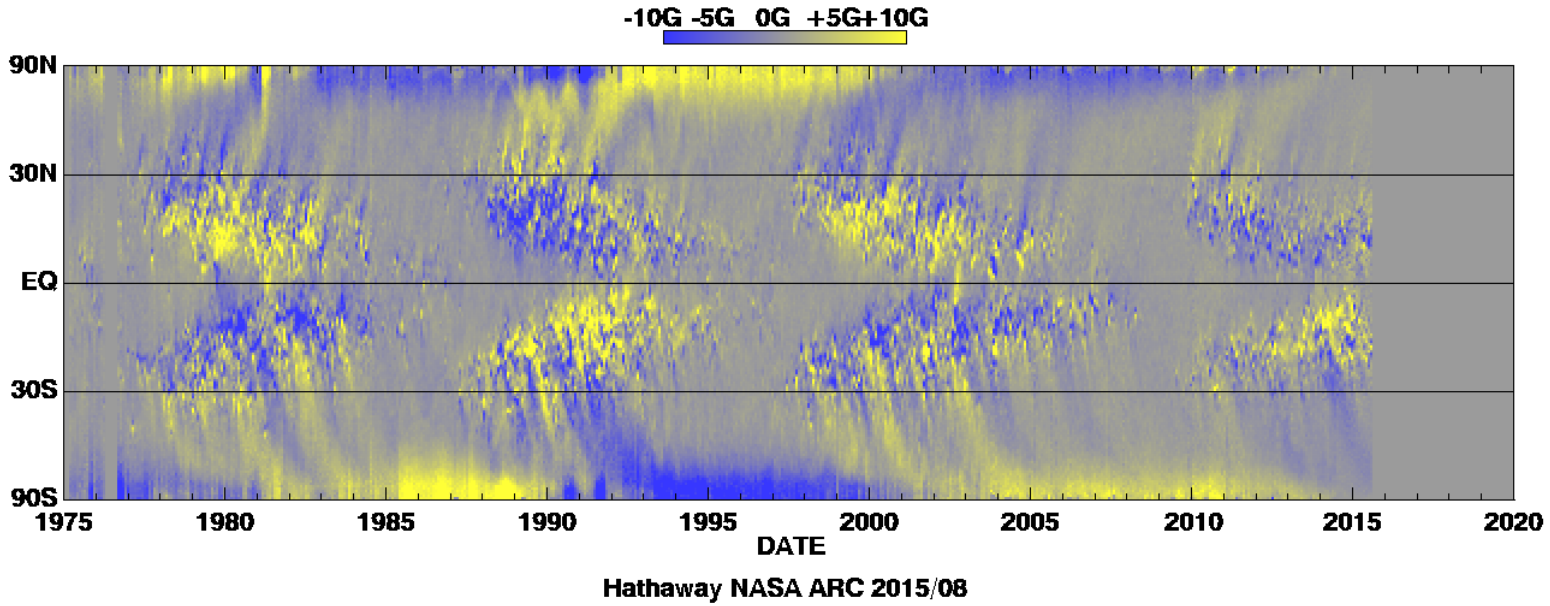

The radial component of the photospheric magnetic field averaged over longitude for each 27-day rotation of the Sun over the last four cycles.

- **Active latitude butterfly wings have following polarity at high latitudes and preceding polarity at low latitudes.**
- **Poleward transport of the predominantly following polarity flux reverses the polar fields at maximum and builds up new polar fields by the next minimum.**

Polar Fields – Producing the next Cycle

Polar Fields at Minimum

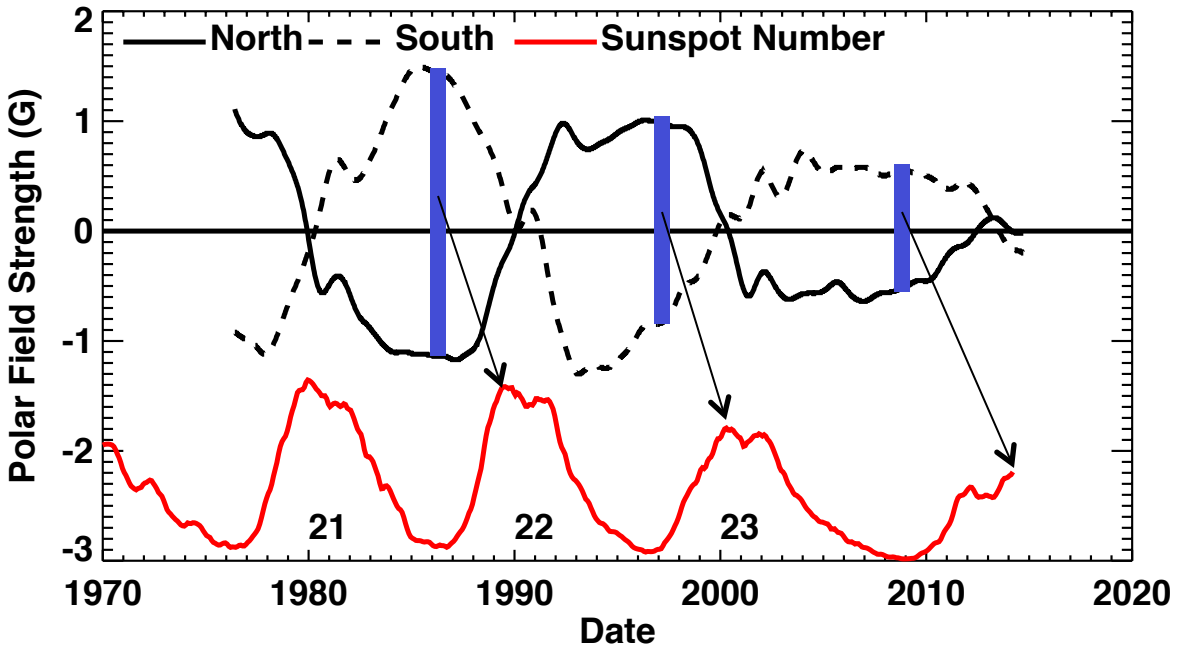

The average polar field strength at cycle minimum (blue bars) correlates well with the maximum sunspot number of next cycle (black arrows).

Polar Field Proxies for Earlier Cycles

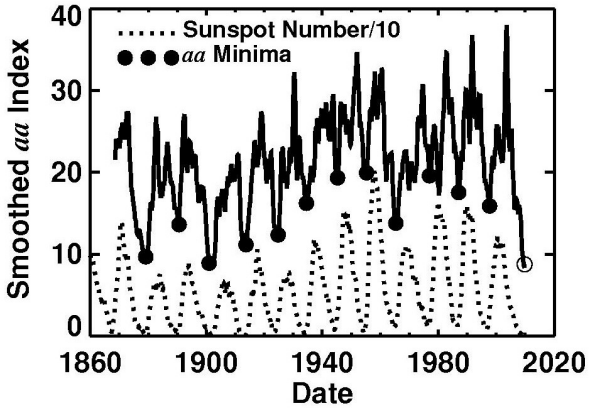

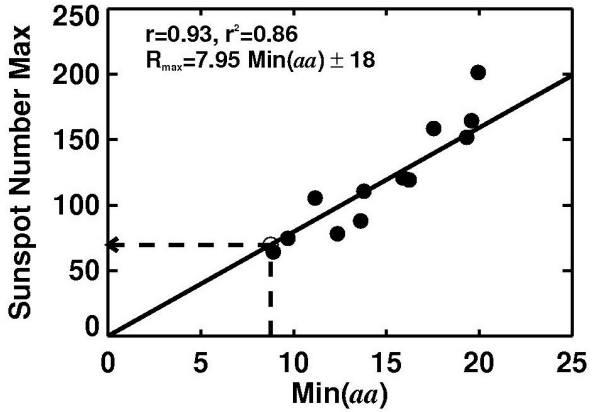

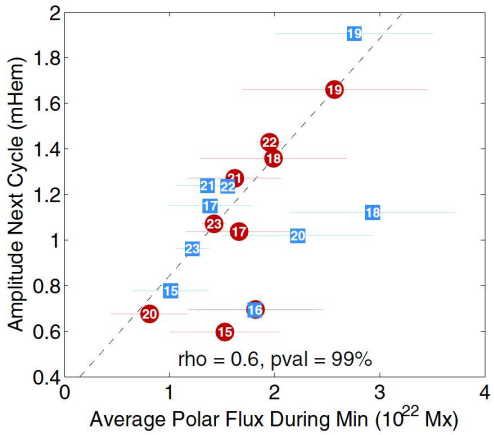

Geomagnetic activity at cycle minima (black dots) is produced by high-speed solar wind streams from coronal holes that carry magnetic fields representative of the dipole field.

The minima in the geomagnetic *aa*-index are well correlated with the maximum sunspot number of the next cycle (Ohl, 1966).

Polar faculae (produced by polar magnetic elements) are well correlated with the maximum sunspot number of the next cycle (Muñoz-Jaramillo et al., 2012).

Surface Flux Transport – Producing the Polar Fields

Surface Flux Transport Observed

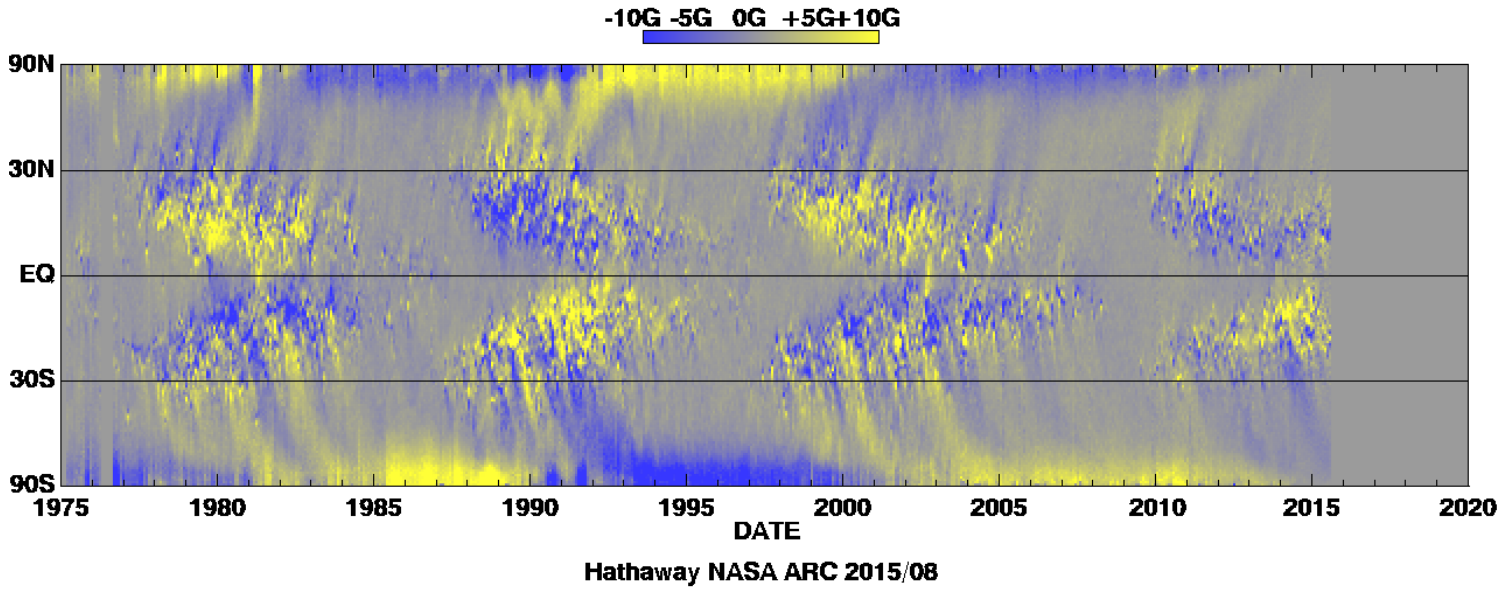

- Active regions emerge with a characteristic tilt that leaves the following-polarity flux at higher latitudes.
- As the cycle progresses active regions emerge at lower and lower latitudes where preceding-polarity flux is canceled and replaced with following-polarity flux.
- This high-latitude, following-polarity flux is transported to the poles by random convective motions and the poleward directed meridional flow.

Surface Flux Transport – Four Decades

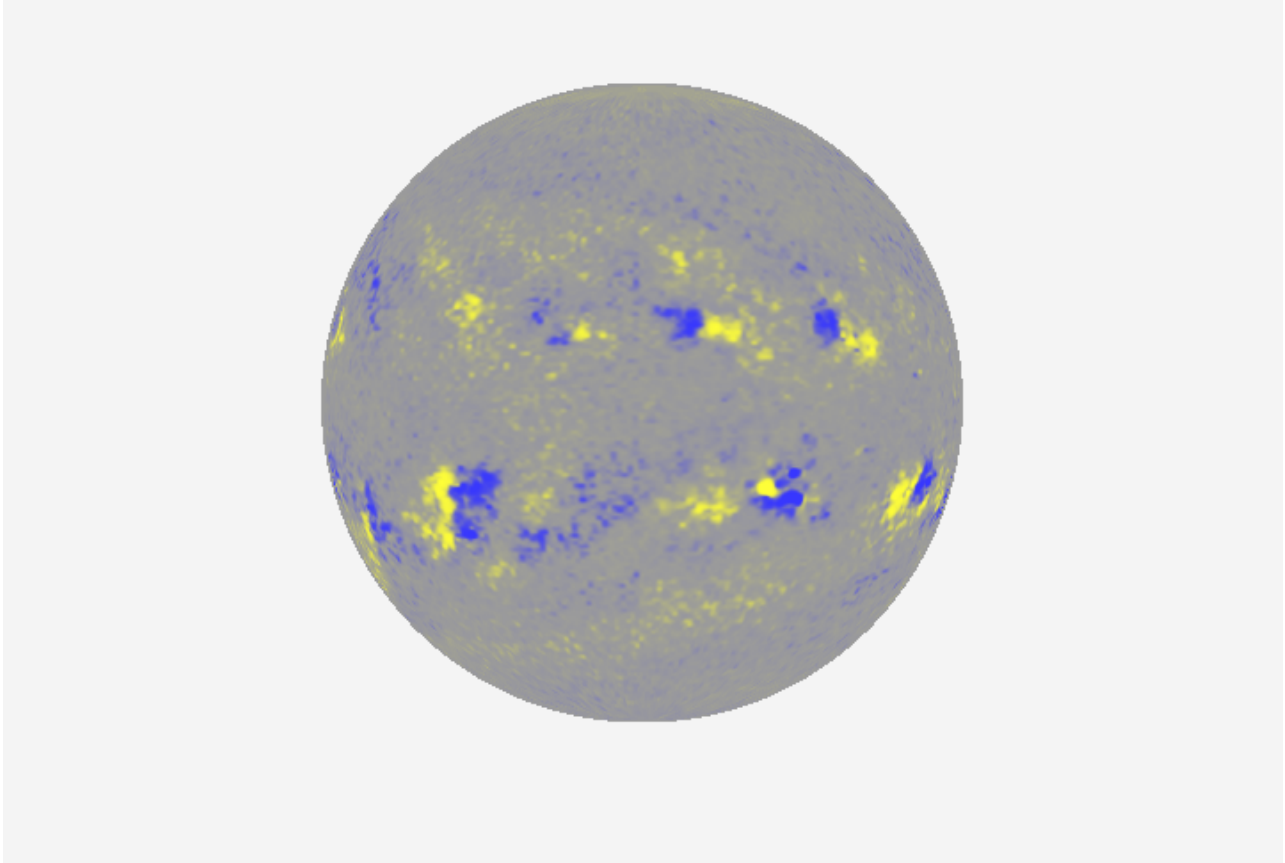

Surface Flux Transport – Four Days

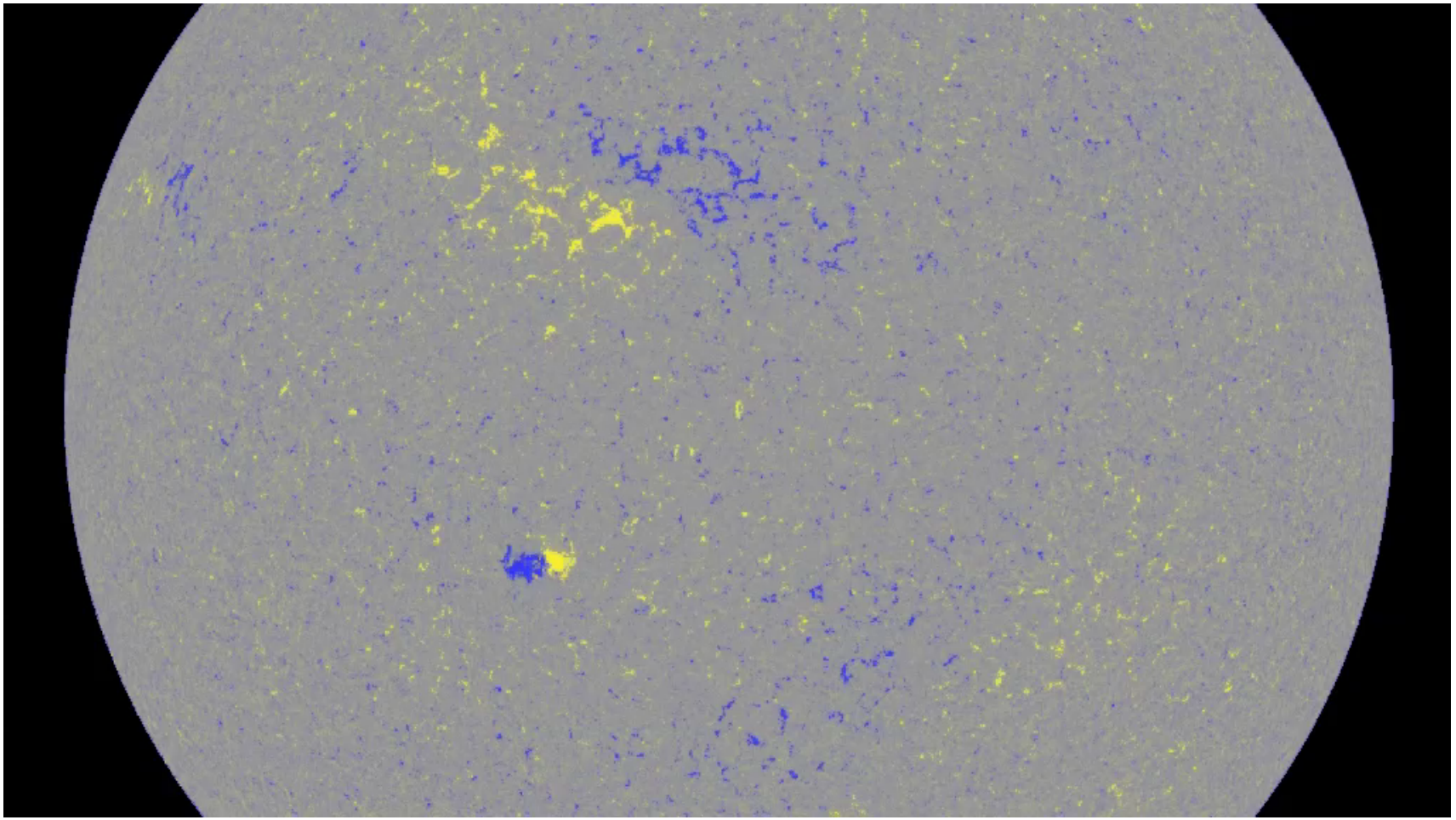

The Surface Flux Transport Promise

The evolution of the Sun's surface magnetic field can be obtained -

1. **Given the emergence of (tilted) active region magnetic flux**
2. **Given knowledge of the flows (the differential rotation, the meridional circulation, the cellular convective flows) and their variations**

Can we use surface flux transport to determine what the strength of the polar fields will be at the cycle minimum well before the end of the cycle?

Measuring the Flux Transport Flows

Correlation Tracking of Magnetic Elements

Full disk magnetograms from SOHO/MDI and SDO/HMI are mapped into heliographic longitude and latitude. Long, narrow strips at each latitude are cross-correlated with similar strips obtained 8 hours later to find the shift in longitude and latitude that gives the best correlation (*Hathaway & Rightmire 2010, 2011*).

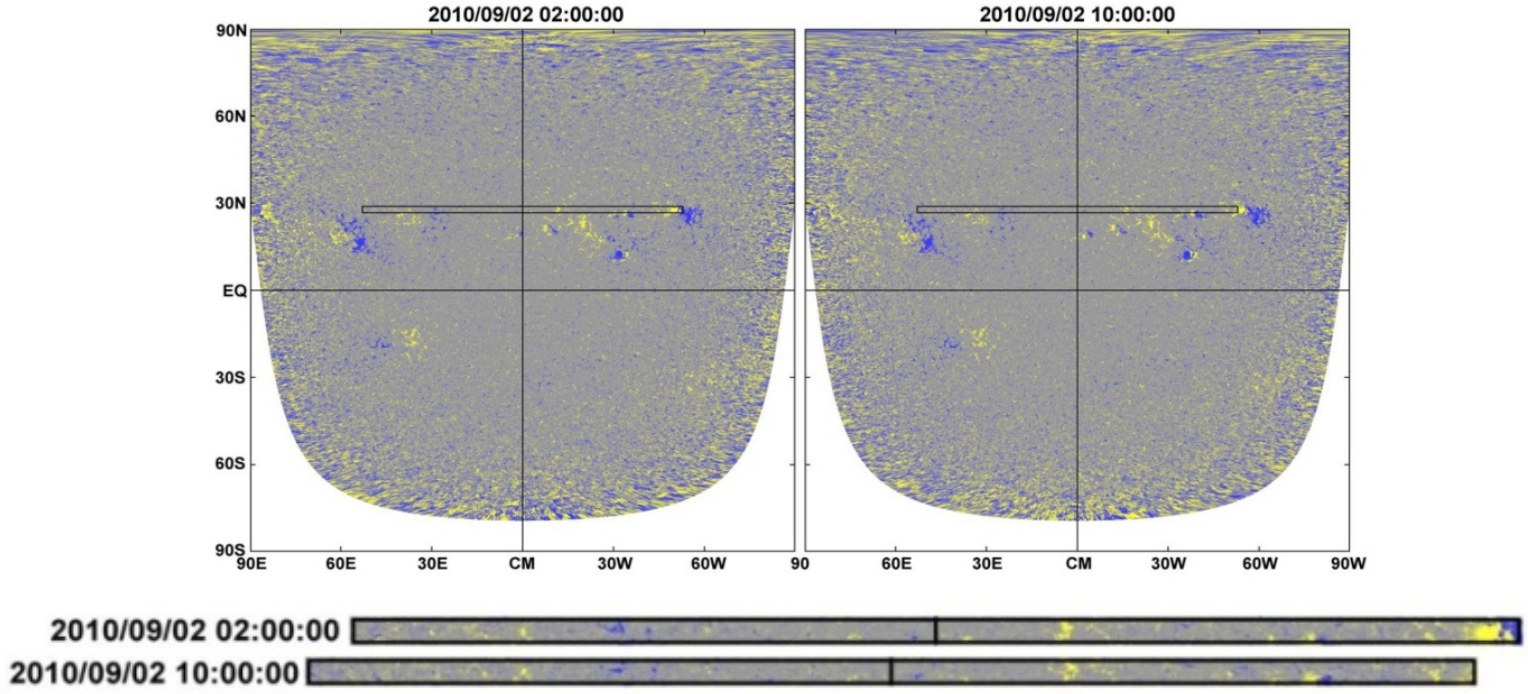

The Differential Rotation

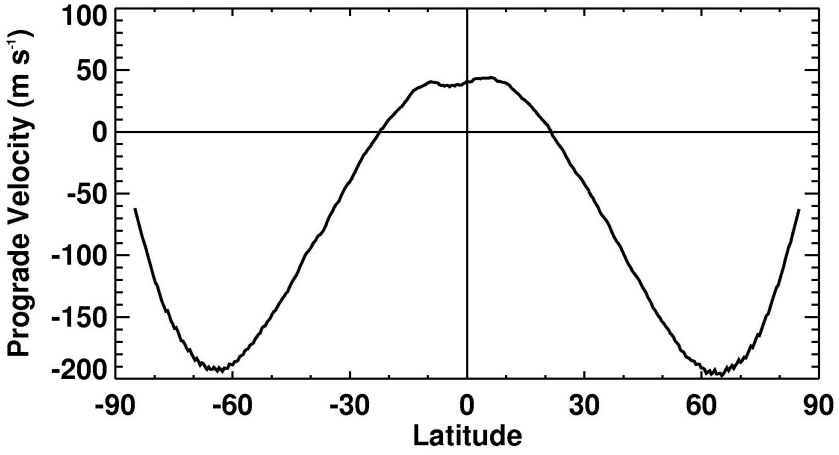

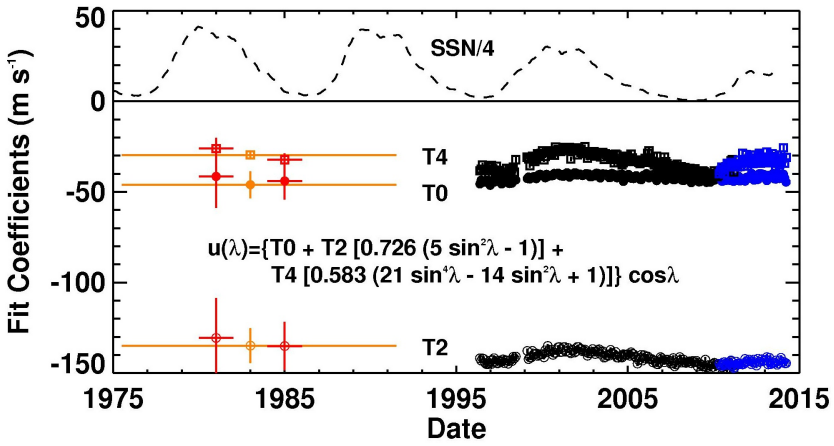

The differential rotation (axisymmetric longitudinal flow) is faster than average at the equator and slower than average at higher latitudes.

We obtained hourly measurements of the latitudinal profiles, averaged them over 27-day solar rotations, and fit the profiles to 4th order polynomials.

Those profiles are well fit with three Legendre polynomials whose coefficients (T_0, T_2, and T_4) vary only slightly with cycle phase – faster and flatter at cycle maximum.

While differential rotation has a huge effect on the longitudinal structure, it does not impact the polar fields.

The Meridional Circulation

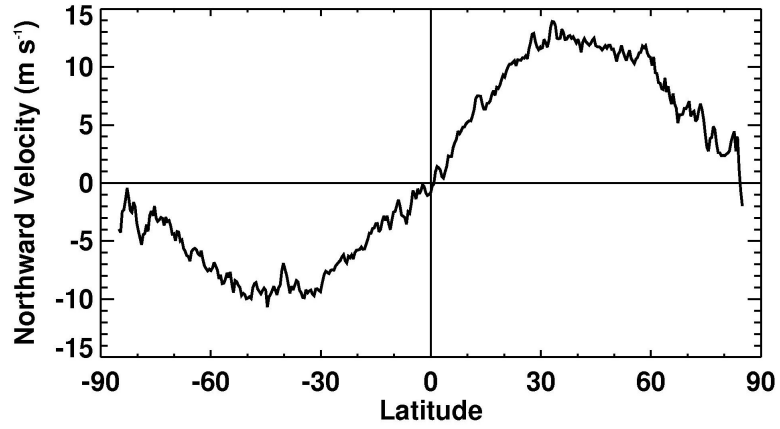

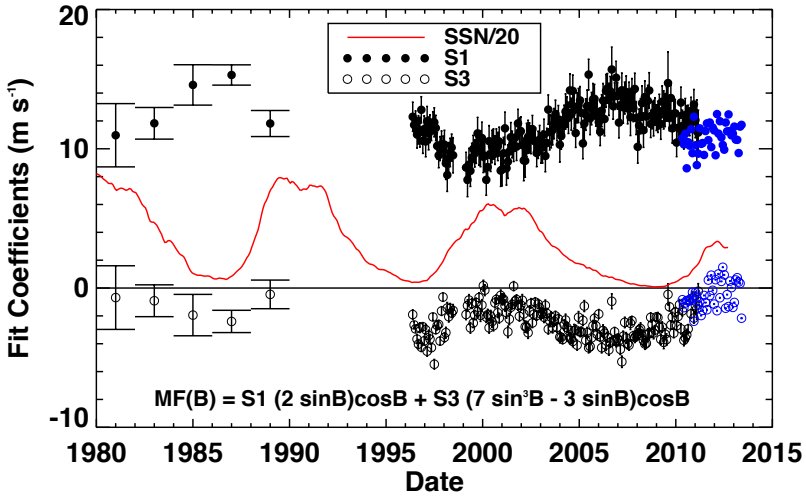

The meridional flow is very weak and has thus been difficult to measure.

The flow is poleward in each hemisphere and peaks at 30-40°.

Measurements with SDO/HMI up to 85° show flow to the poles without any evidence for counter-cells at high latitudes.

The meridional flow profiles are well fit by two Legendre polynomials with coefficients S_1 and S_3.

Our measurements (and earlier measurements by *Komm, Howard, & Harvey, 1993*) show that the flow is fast at cycle minima, slow at cycle maxima, and varies from cycle to cycle.

Deviations from the Average

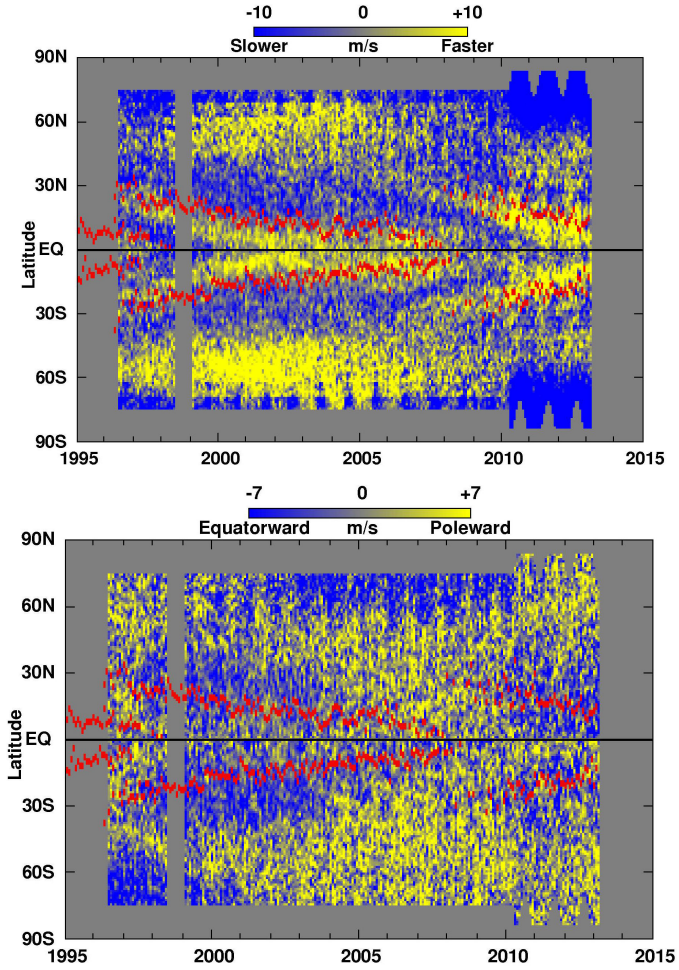

Removing the average differential rotation profile from the profiles for each individual solar rotation reveals the "Torsional Oscillations" – faster rotation on the equatorward sides of the active latitude bands (red dots indicate sunspot area centroids) and slower rotation on the poleward sides.

The high-latitude spin-up around the time of cycle maximum produces the faster rotation and flatter rotation profiles at maxima.

Removing the average meridional flow profile from the profiles for each individual solar rotation reveals "Active Latitude Inflows" – poleward flow on the equatorward sides of the active latitudes and equatorward flows on the poleward sides.

These inflows produce the weaker meridional flow at cycle maxima and they vary with the level of activity in a cycle.

The Convective Flows

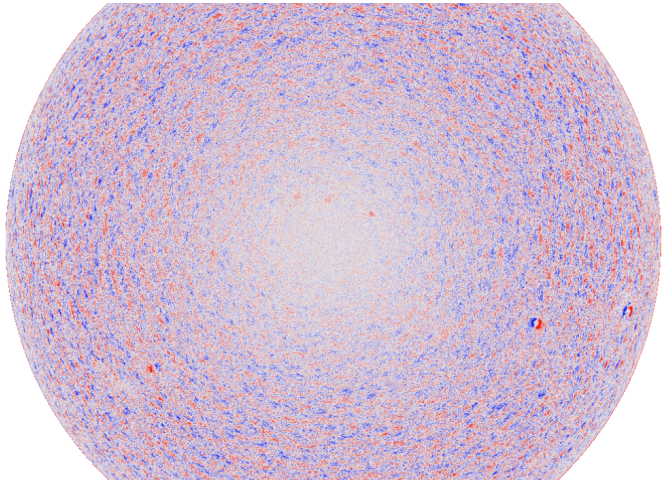

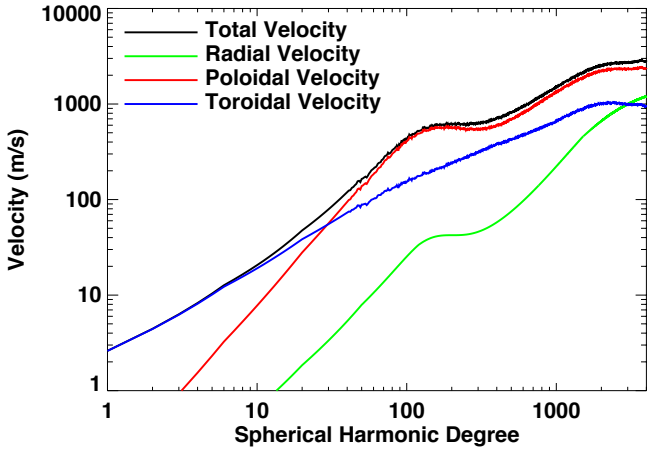

Hathaway et al. (2015) **analyzed and simulated Doppler velocity data from SDO/HMI to determine the spectrum of flow velocities for all three vector velocity components – radial velocity, poloidal velocity (horizontal flows with divergence), and toroidal flows (horizontal flows with curl).**

The total velocity increases with wavenumber to a peak of ~500 m/s for cells the size of supergranules (30 Mm in diameter) and then rises again to a peak of ~3000 m/s for cells the size of granules (1200 km in diameter).

Toroidal (heliostrophic?) flows dominate at wavenumbers less than 30.

There is only weak evidence for changes in the spectrum with the solar cycle.

Giant Cells

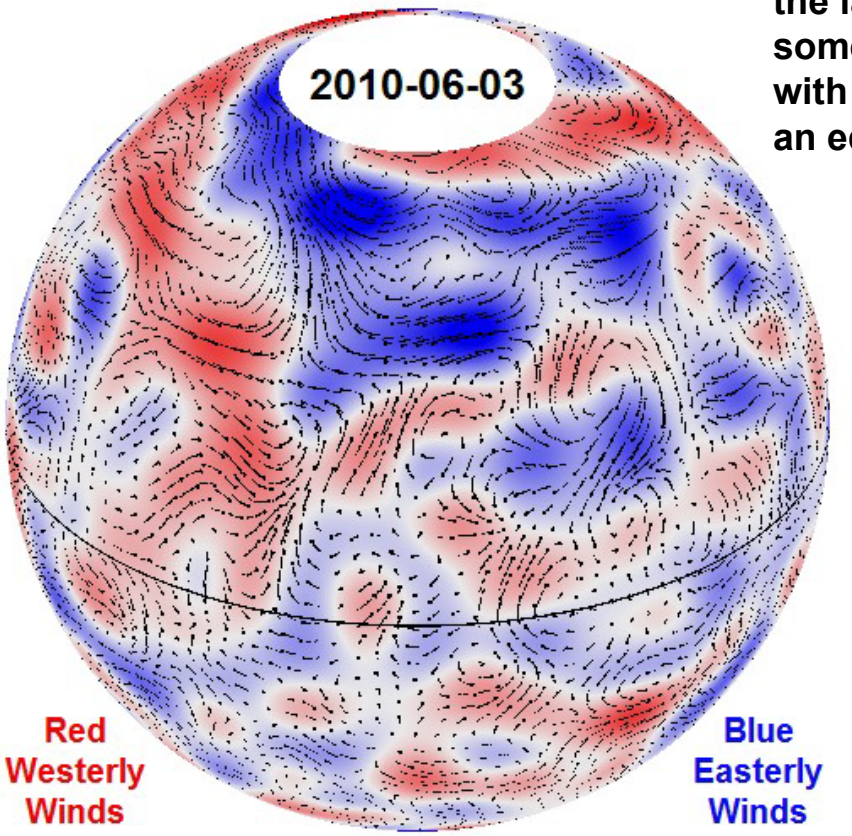

Hathaway, Upton, & Colegrove (2013) **found that the largest cellular flow structures on the Sun had some expected flow properties – cyclonic flows with hemisphere dependent kinetic helicity and an equatorward flux of zonal momentum**

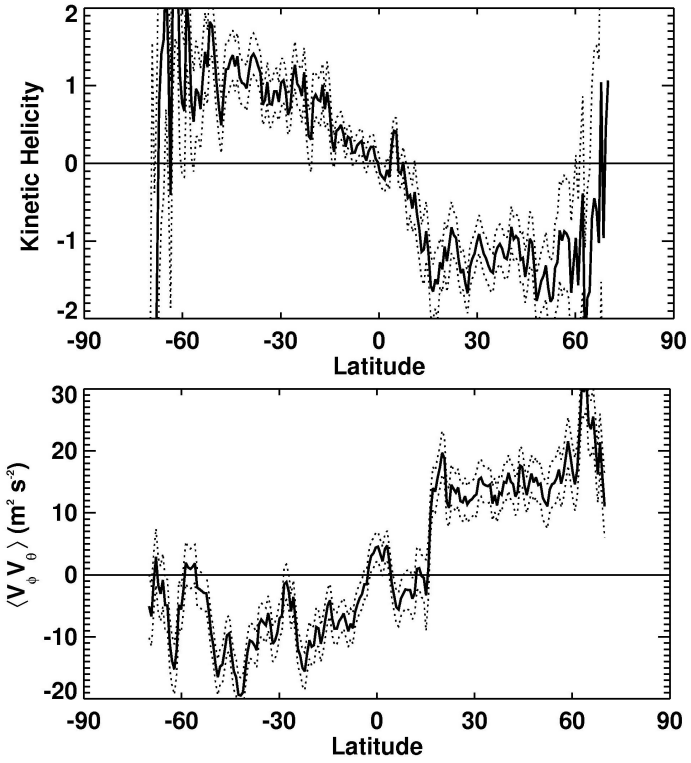

The Full Convection Spectrum

The velocity spectrum from our analysis of SDO/HMI Doppler velocity data agrees well with the spectrum of the "Giant Cells" from supergranule correlation tracking at the low wavenumber end (black line), and also agrees well with the spectrum of the flows in the StellarBox Radiative-MHD simulation of *Wray et al. (2015)* at the high wavenumber end (blue).

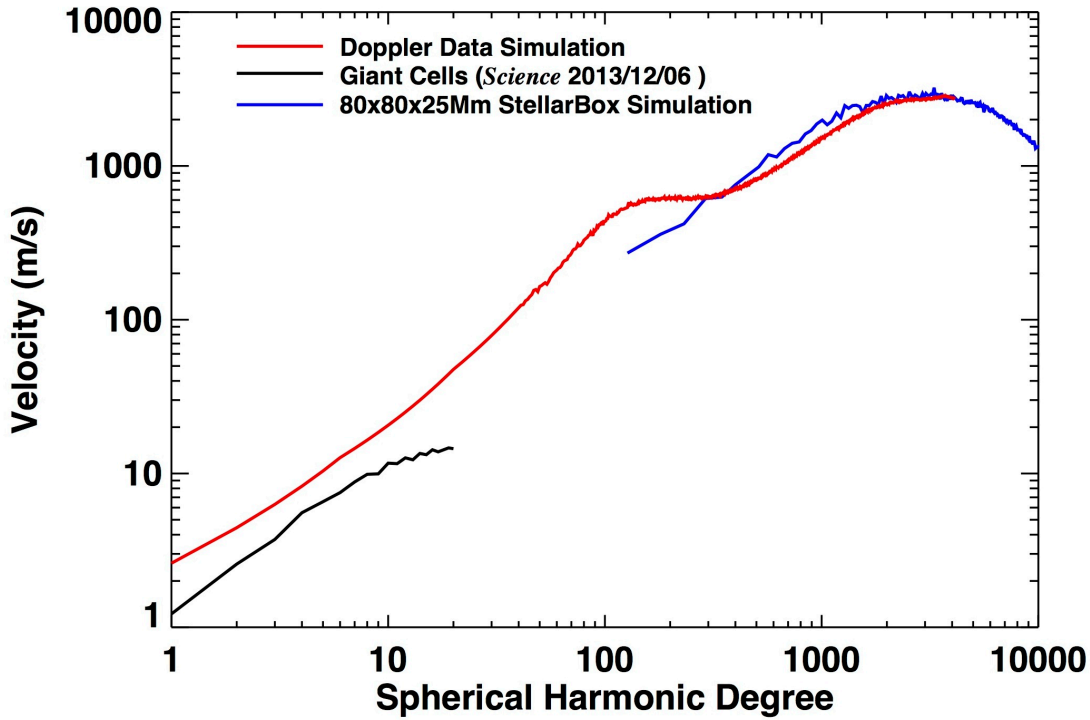

Reconstructing and Predicting the Cycle

Advective Flux Transport (AFT) Code

Kinematic model – flows are specified, transport is of a passive scalar (radial component of the magnetic field)

Refined rectangular grid in longitude and latitude (512 equispaced nodes in latitude, 1024cos*(latitude) equispaced nodes in longitude at each latitude rounded up to next power of 2)**

Flows are calculated from an evolving spectrum of vector spherical harmonics in FORTRAN with 4^{th} order Runga-Kutta time stepping (evolution is due to advection of the convective flows by the axisymmetric flows and random complex phase perturbations to give lifetimes)

Flux transport and data assimilation are calculated in IDL (explicit 1^{st} order time steps of 300s, diffusive term added to minimize Gibbs ringing around flux concentrations, quenching of convective flows in active regions)

Kalman Filtering made Simple

Predicted field from model	$B'(\phi,\theta,t_k) = f(B(\phi,\theta,t_{k-1}), v(\phi,\theta,t_{k-1}))$ [via the AFT code]	
Model uncertainty	$W'(\phi,\theta,t_k) = W(\phi,\theta,t_{k-1}) + U_m$	[U_m = 1.0 everywhere]
Data Uncertainty	$U_d(\phi,\theta,t_k) = a/\cos^n\rho$	[a=100 n=4]
Kalman Weight	$K(\phi,\theta,t_k) = W'(\phi,\theta,t_k) / (W'(\phi,\theta,t_k) + U_d(\phi,\theta,t_k))$	
New Field values	$B(\phi,\theta,t_k) = K(\phi,\theta,t_k)\, Z(\phi,\theta,t_k) + (1 - K(\phi,\theta,t_k))\, B'(\phi,\theta,t_k)$	
	$Z(\phi,\theta,t_k)$ = New Observations	
New Model uncertainty	$W(\phi,\theta,t_k) = (1 - K(\phi,\theta,t_k))\, W'(\phi,\theta,t_k)$	

We use: a=316 for MDI 1-minute data, a=100 for MDI 5-minute data, a=100 for HMI 12-minute data

Magnetic Map Data Assimilation

Kalman Filtering Method

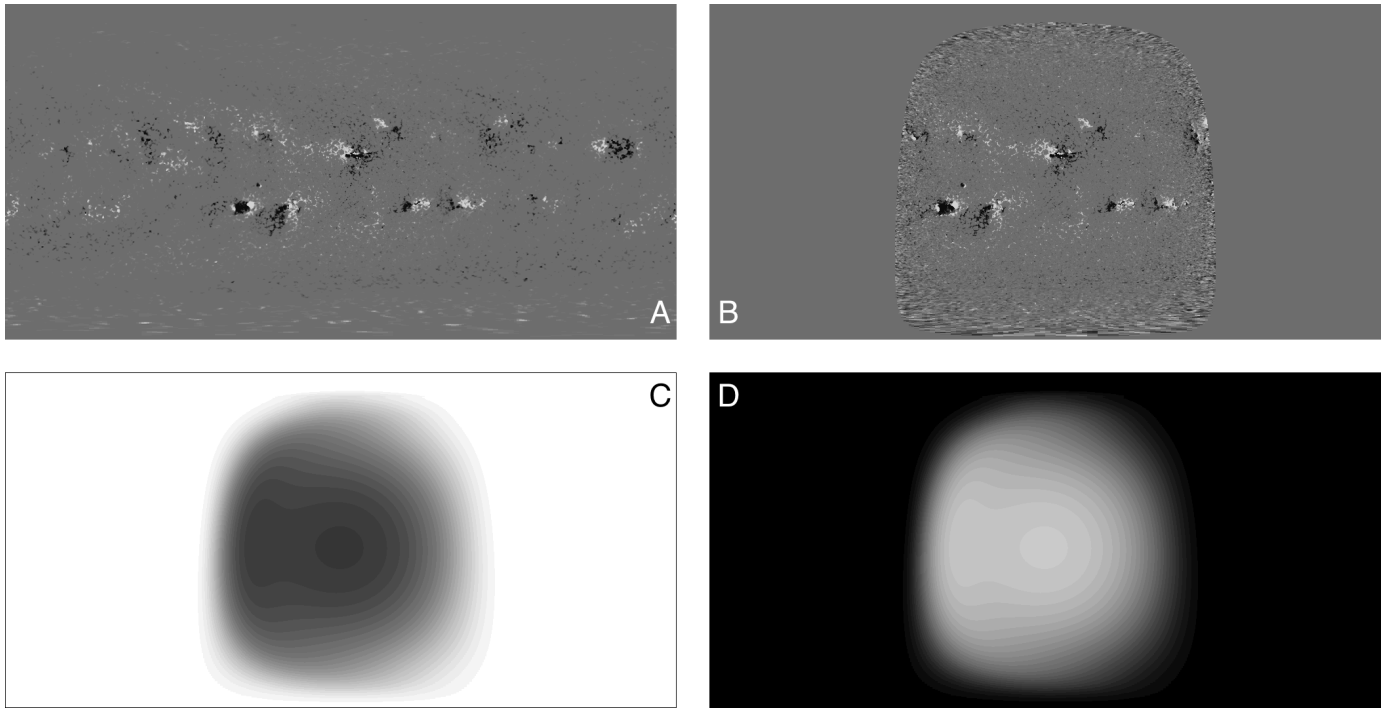

A) Updated model map, $B'(\phi,\theta,t_k)$. B) Current magnetogram, $Z(\phi,\theta,t_k)$. C) The weights for the model data, $(1 - K(\phi,\theta,t_k))$. D) The weights for the current data, $K(\phi,\theta,t_k)$.

New Map = A*(1 – D) + B*D

With Full-Disk Data Assimilation

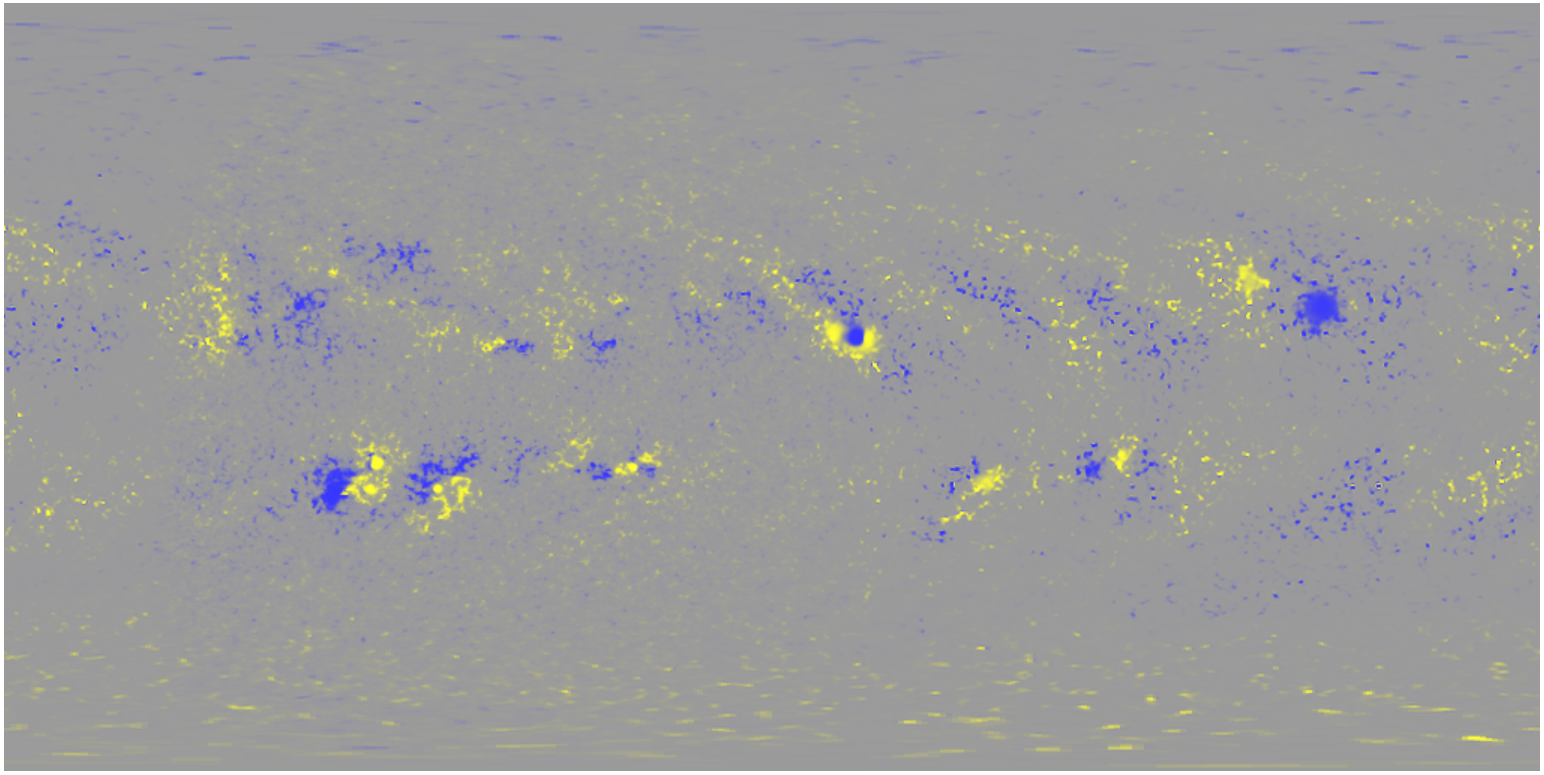

With Active Region Sources Only

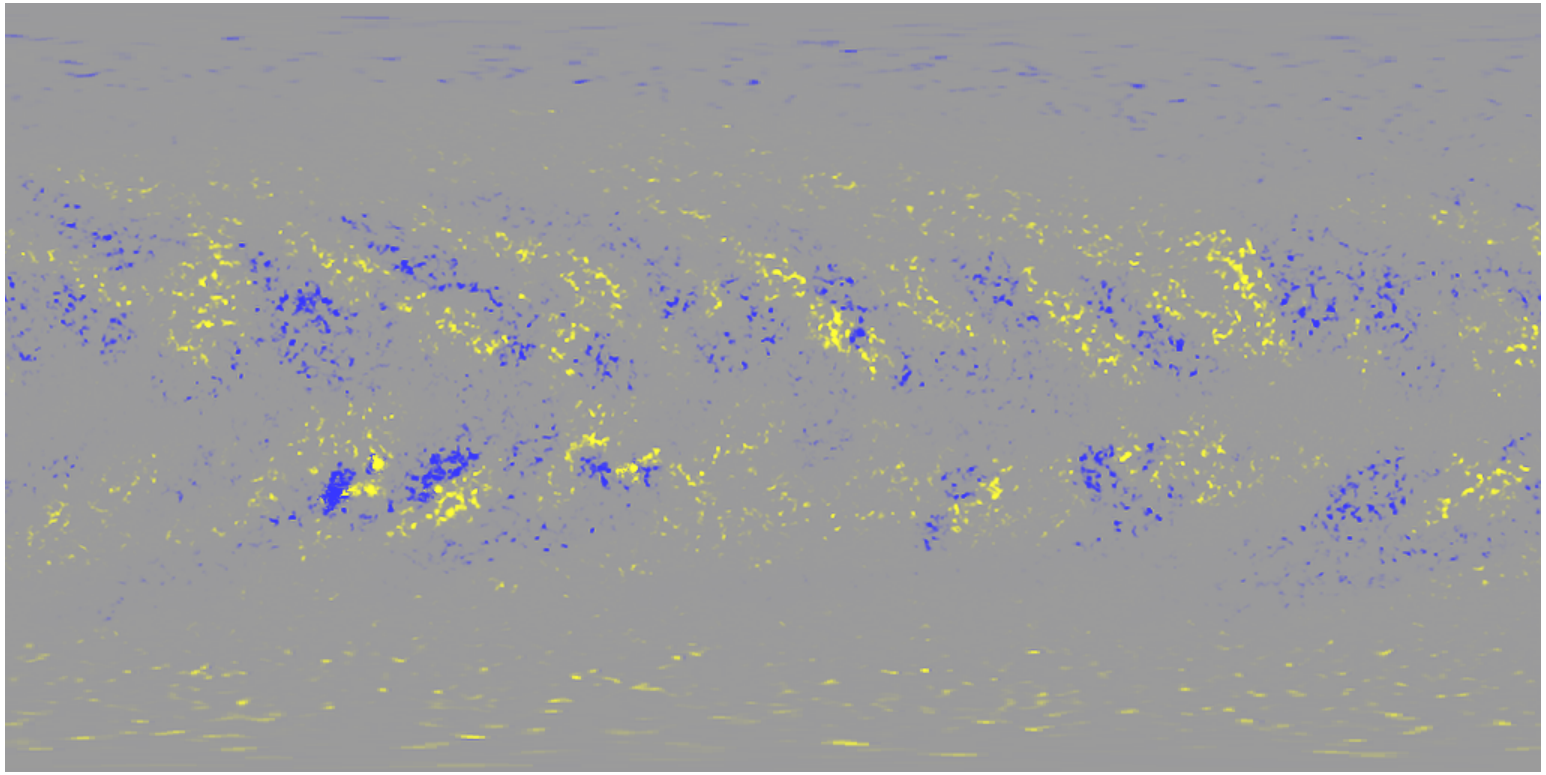

Testing the Flux Transport Promise

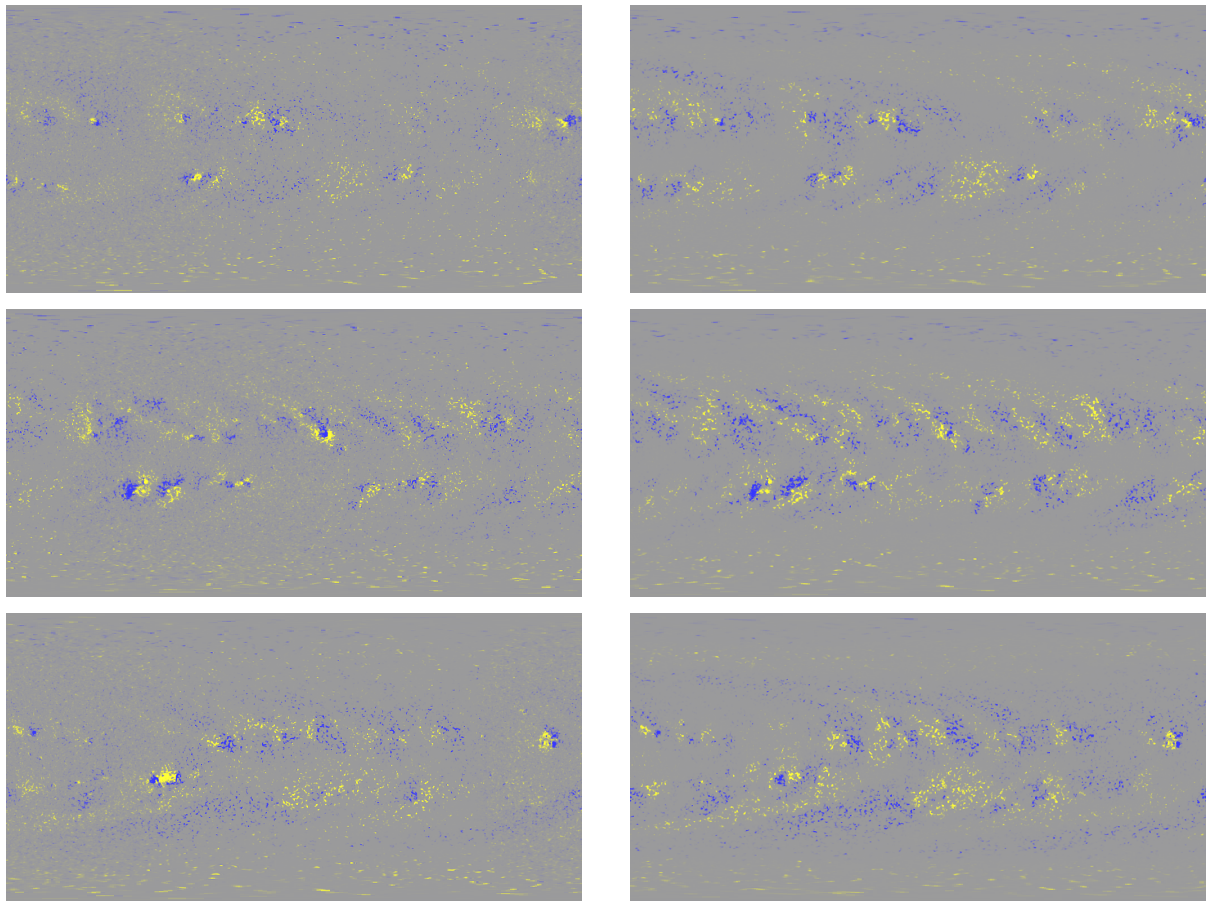

Longitudinal Averages

Full-disk
Data assimilation

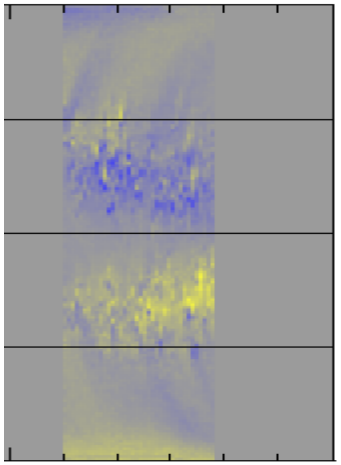

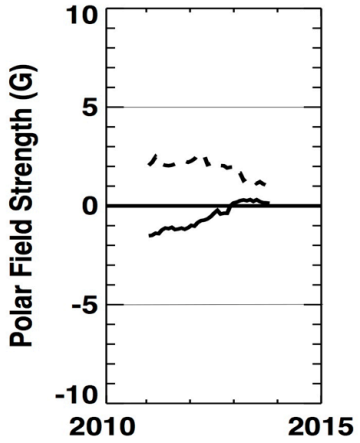

Active Region
Sources

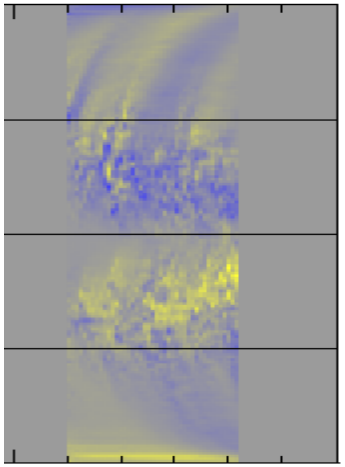

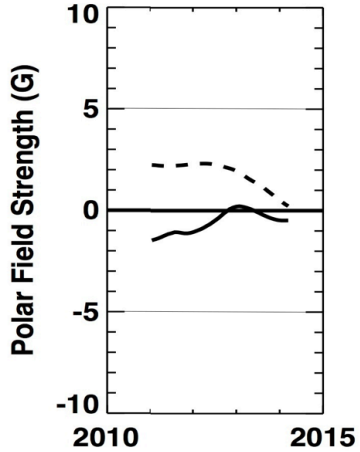

Predicting Polar Fields

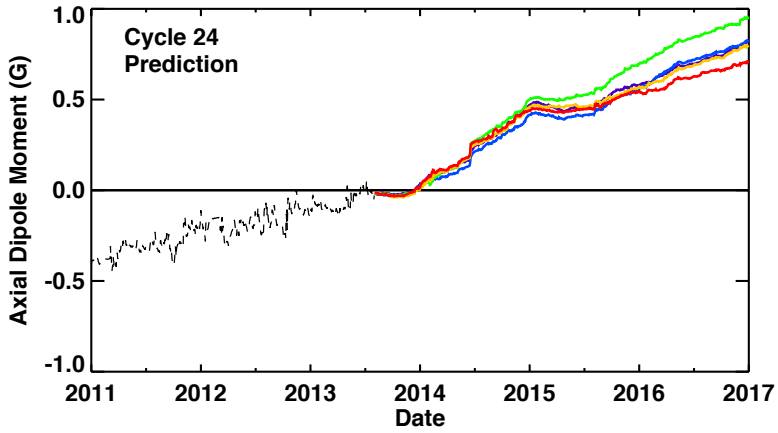

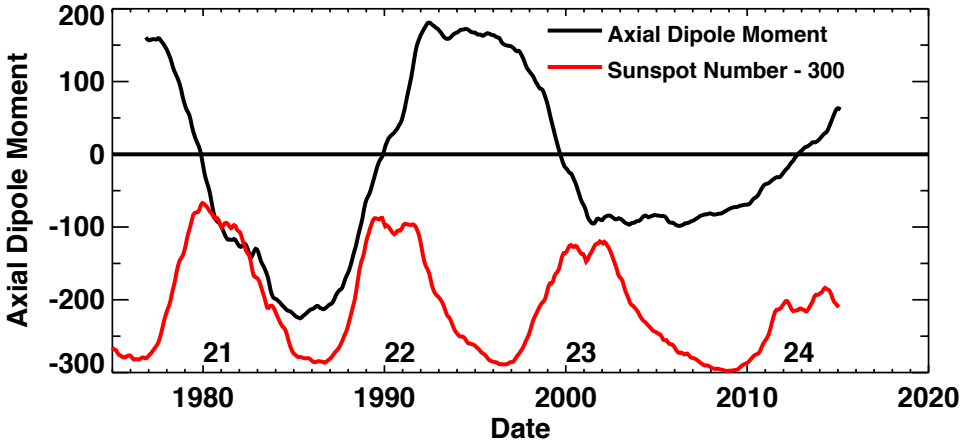

Our (*Upton & Hathaway, 2013*) polar field prediction based on surface flux transport using active region sources from cycle 14 (a similar cycle) shows good agreement.

The axial dipole moment measured by the Wilcox Solar Observatory shows the reversal in early 2013 and a rise to absolute values near those seen in early 2011 by early 2015.

Note: Using different realizations of the convective motions (multi-colored tracks) gives diverging results - e.g. axial dipole = 0.8 ± 0.1 after 3.5 years.

Cycle 23 and Meridional Flow Variations

Upton & Hathaway (2014) **showed that the observed variations in the meridional flow during cycle 23 produced stronger polar fields than would be produced with a constant, average, meridional flow profile.**

This suggests that the changes to the meridional flow induced by the presence of active regions modulates the cycle amplitudes (*Cameron & Schüssler, 2012*).

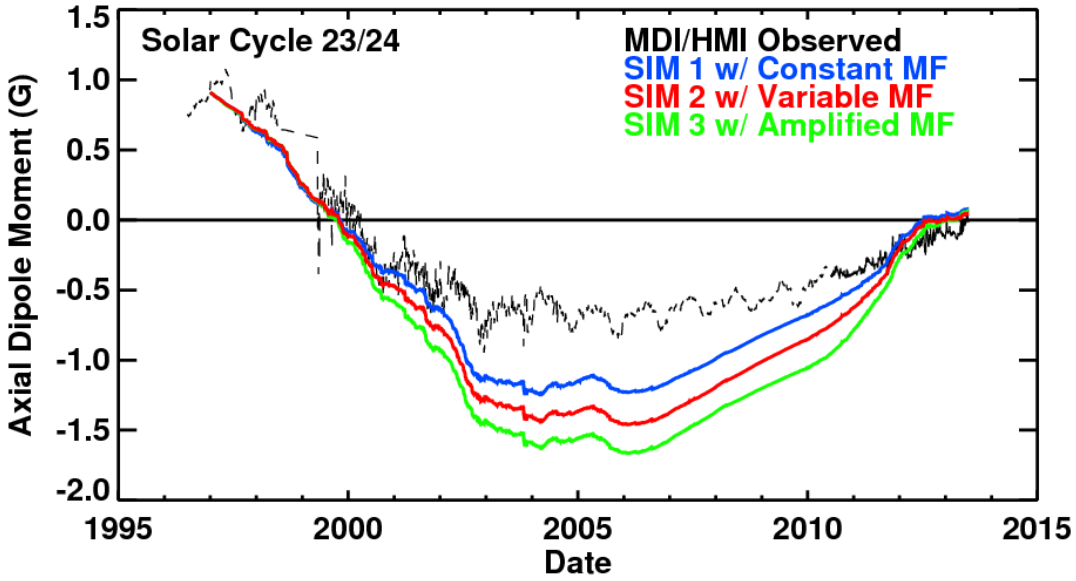

Note: Changes in the meridional flow can produce significant changes in the results – e.g. axial dipole maximum = 1.4 ± 0.2.

Active region Tilt Variations

Cameron et al. (2013) **noted that the emergence of just a few badly oriented active regions can have significant consequences for the polar fields.**

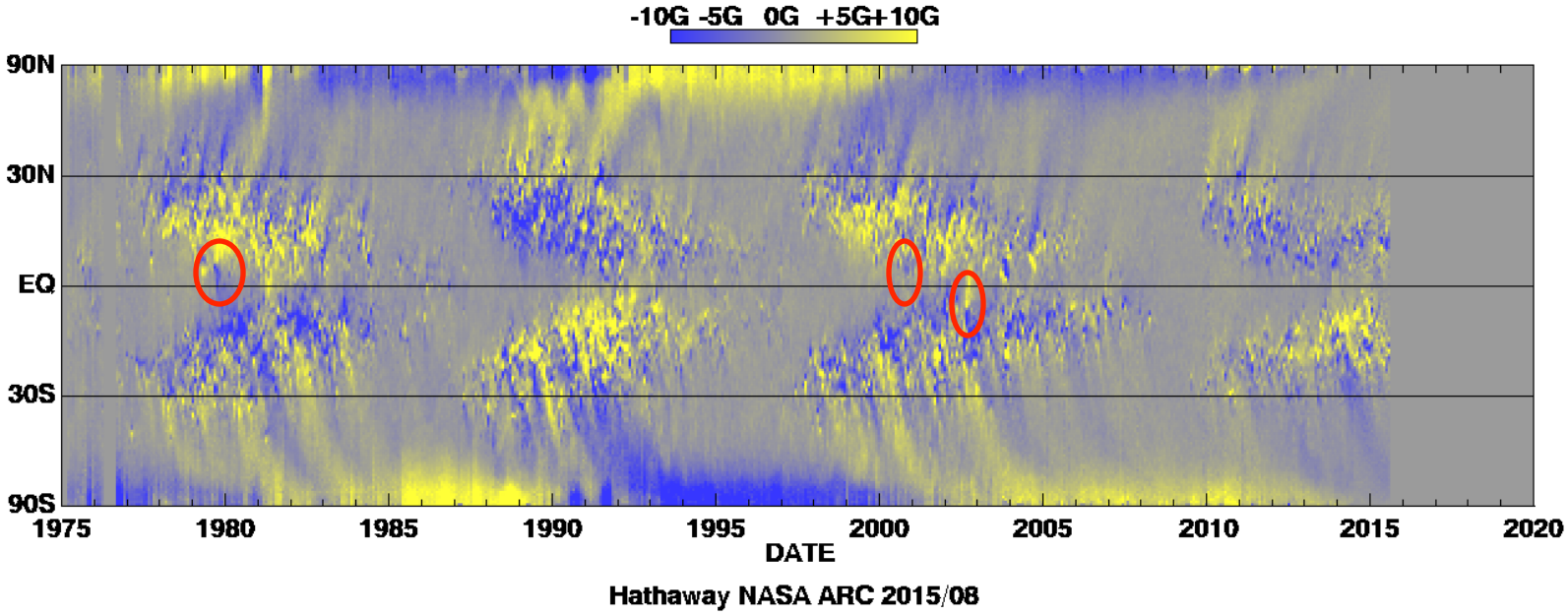

Note: Random perturbations in the tilt of large active regions can alter the axial dipole.

Spherical Harmonic Flux Transport Code

We (Thomas Hartlep, Nagi Mansour, and myself) have developed a new flux transport code using spherical harmonics for both the flows and the transport with 4th order Runga-Kutta time stepping

Improved Kalman filtering for data assimilation

Improved velocity quenching in active regions

Far-side active region development from *STEREO* Mission EUV images

Conclusions

- We can predict the level of activity in an ongoing cycle once a cycle is well underway (curve-fitting)
- We can predict the amplitude and timing of a future cycle based on observed polar fields at the time of minimum
- We can predict polar fields at least 2-3 years ahead based on surface flux transport with active region sources based on statistics
- Long range predictions (more than one cycle ahead) are limited by:
  1. Random variations in the convective flows
  2. Future variations in the meridional flow
  3. Random variations in the tilt of active regions

Caveat Emptor